Exciton energy transfer between asymmetric quantum wires: Effect of transfer to an array of wires

S. K. Lyo
*Sandia National Laboratories, Albuquerque, New Mexico 87185, USA**
and Korea Advanced Institute of Science and Technology (KAIST), Taejon, South Korea
(Received 17 January 2006; published 11 May 2006)

We study the Stokes exciton transfer rate from a narrow quantum wire (QWR) to a parallel wide QWR separated by a wide barrier and also to a planar array of parallel wide QWRs. The transfer rate is calculated as a function of the distance d between the narrow QWR and the wide QWR and also the array. The dependence of the rate on the temperature and the localization radius is studied for free and localized excitons, respectively. Both the resonant and nonresonant rates are considered. We find that, for energy transfer between two QWRs, the Förster dipole-dipole transfer dominates the transfer rate at short and intermediate distances. The photon-exchange transfer prevails only at an extremely long distance where the rate is negligibly small. This behavior is in contrast with the two-dimensional quantum wells, where the photon-exchange mechanism is dominant except at a very short distance. However, for the energy transfer to an array of QWRs, the photon-exchange transfer rate continues to increase as the array size grows to a macroscopic scale due to its slow range dependence while the dipolar rate saturates quickly with the array size. As a result, the photon-exchange transfer can become dominant in a system consisting of stacks of QWRs or arrays distributed over a wide range. The prediction of the theory is consistent with recent data from V-groove GaAs/$Al_xGa_{1-x}As$ double quantum wires.

DOI: 10.1103/PhysRevB.73.205322 PACS number(s): 71.35.−y, 71.35.Cc, 78.67.Lt, 78.55.Cr

I. INTRODUCTION

Excitons are a useful storage reservoir of light energy and play an important role in optical devices. Modern semiconductor device structures contain stacked two-dimensional (2D) layers and one-dimensional (1D) wires for an increased efficiency. The physics of exciton motion between these confined structures is not yet satisfactorily understood and is of much practical and academic interest. While exciton transfer between 2D quantum wells (QWs) have been studied in the past experimentally[1,2] and theoretically,[1,3,4] exciton transfer between 1D quantum wires (QWRs) is attracting attention only recently[5] due to the difficulty of growing these structures. In this paper, we present a study of the Stokes energy transfer rate from a narrow QWR (nQWR) to a wide QWR (wQWR). This transition has been observed recently between two V-groove GaAs QWRs.[5] The anti-Stokes rate from a wide well to a narrow well is expected to be much slower[1] for a large energy mismatch because it involves higher-order inelastic processes and is more difficult to observe. This rate relies on a different mechanism[3] and is beyond the scope of the present treatment. We also study energy transfer from a nQWR to an array of parallel wQWRs as a function of the array size and the distance between the nQWR and the array.

According to previous data,[1,2] the exciton transfer rate between widely separated 2D QWs decays slowly with the distance between the QWs, persisting over a surprisingly long distance, over many tens of micrometers. This intriguing behavior could not be explained[1–3] by the standard Förster[7] (e.g., dipole-dipole) transfer rate which decays rapidly as $\propto 1/d^4$, where d is the center-to-center distance between the QWs. This behavior was explained recently by the present author by showing that while the Förster mechanism dominates the rate at a very short distance (<10 nms), the photon-exchange coupling prevails at a longer distance.[3] This result arises from the fact that the photon-exchange coupling decays slowly with distance and that photons can reach a wide area in the target (i.e., final-state) QW, enhancing the efficiency.[8] In the present 1D-1D transfer problem, however, the target QWR has a small effective cross section due to the narrow dimension in the direction perpendicular to the plane containing both wires, resulting in a poor efficiency for the long-range photon-exchange mechanism compared with the 2D-2D case. For the energy transfer between the nQWR and an array of wQWRs, however, the photon-exchange transfer rate is shown to continue to increase slowly as the array size grows to a macroscopic scale in contrast with the dipole-dipole rate which is shown to saturate quickly with the increasing array size. As a result, the photon-exchange transfer becomes important in a system consisting of stacks of QWRs or arrays distributed over a wide range. For energy transfer between two parallel QWRs, the prediction of this paper is consistent with the recent data[5] which showed that the rate decays rapidly as a function of d. The same data,[5] however, show a slow decay of the rate with increasing d for transfer between 2D QWs in agreement with earlier data.[1,2] In the present paper, we extend our previous work,[3] presenting the essential formalism relevant for the 1D-1D transfer.

The organization of the paper is as follows. In the next section, we present a basic formalism describing the 1D exciton states and the electron-hole (e-h) pair states. The exciton transfer mechanism through dipole-dipole coupling and photon-exchange interaction is described in Sec. III. The transition rate is given in Sec. IV. In Sec. V we discuss the basic approximations employed for evaluating the rate. The

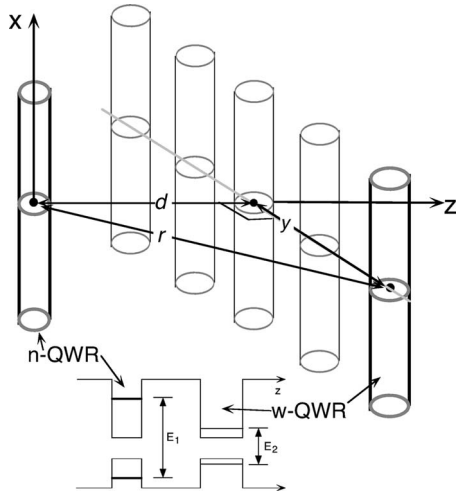

FIG. 1. A schematic diagram of two narrow and wide QWRs (bold figures) parallel to the x axis. The two wires are separated by the center-to-center distance $d(y)$ in the $z(y)$ direction. The wires in the background represent a uniform symmetric planar array of identical parallel wide wires. The inset at the bottom shows the ground sublevels of the nQWR (thick horizontal lines) and the wQWR (thin horizontal lines) in the conduction and valence bands in the z direction. The energy mismatch is given by $E_{12}=E_1-E_2$.

transfer rates are numerically evaluated in Sec. VI, where discussions of the results and a comparison with recent data are presented. Finally, a brief concluding remark is given in Sec. VII.

II. BASIC FORMALISM

The two QWRs of interest are shown schematically by the two cylindrical wires in bold figures in Fig. 1. They are separated by a distance d in the z direction and y in the y direction with a net distance $r=\sqrt{d^2+y^2}$. The wires are along the x direction. Numerical studies for transfer between two QWRs are carried out for $y=0$, namely for $r=d$ while the formalism is given for general y. The rest of the wires in Fig. 1 are identical to wQWR and form an array parallel to the x-y plane. Energy transfer from the nQWR to the array structure will be considered later. The confinement is assumed to be strongest in the z direction and only the ground sublevels shown in the bottom inset are relevant in this direction. Experimentally, the illustrated structure is a rough approximation to parallel V-groove quantum wires.[5] The excitons are initially in the ground sublevel of the nQWR and transfer to the ground sublevel of the wQWR, which is much lower in energy as illustrated in the lower inset of Fig. 1. This nonresonant transfer is dominantly via e-h pair emission. It is possible that one of the sublevels of the wQWR in the y direction may be close to the ground level of the nQWR. In this case, resonant transfer can be efficient.

The $1s$ exciton wave function in the jth ($j=1,2$) QWR is given by[3,6]

$$|j,K\rangle = \frac{v_0}{\sqrt{L}} \sum_{\mathbf{r}_e,\mathbf{r}_h} e^{iKX} F_j(x,\mathbf{r}_{e\perp}-\mathbf{r}_{j\perp};\mathbf{r}_{h\perp}-\mathbf{r}_{j\perp}) a^\dagger_{c\mathbf{r}_e} a_{v\mathbf{r}_h}|0\rangle, \tag{1}$$

where K is the wave number for the center-of-mass (CM) motion, $X=\alpha_e x_e+\alpha_h x_h$ is the CM coordinate along the wire, $x=x_e-x_h$ is the relative coordinate, $\mathbf{r}_\sigma=(x_\sigma,\mathbf{r}_{\sigma\perp})$ is the position of the electron ($\sigma=e$) and the hole ($\sigma=h$), $\mathbf{r}_{j\perp}$ is the position of the jth QWR in the direction perpendicular to the wire, $\alpha_\sigma=m_\sigma/M$, and $M=m_e+m_h$ is the total mass. We assume that the indices $j=1$ and 2 represent the nQWR and the wQWR, respectively. In Eq. (1), L is the wire length, v_0 is the unit-cell volume, and $|0\rangle$ signifies the ground state with an empty conduction band and a filled valence band. The creation and destruction operators $a^\dagger_{c\mathbf{r}_e}$ and $a_{c\mathbf{r}_e}$ ($a^\dagger_{v\mathbf{r}_h}$ and $a_{v\mathbf{r}_h}$) creates and destroys an electron in the conduction (valence) band at the position $\mathbf{r}_e$ ($\mathbf{r}_h$) in the Wannier representation. The normalization condition of the wave function is given by $\langle j',K'|j,K\rangle=\delta_{j,j'}\delta_{K,K'}$ or equivalently by

$$\int dx \int d^2r_{e\perp} \int d^2r_{h\perp} |F_j(x,\mathbf{r}_{e\perp};\mathbf{r}_{h\perp})|^2 = 1, \tag{2}$$

as can be shown by converting $\Sigma_{\mathbf{r}_\sigma}\to\int d^3r_\sigma/v_0$. Here, the overlap between the confinement wave functions of the two QWRs is neglected.

Excitons can be localized due to disorder such as introduced by interface roughness. In this case, we introduce a phenomenological (normalized) wave function for the CM coordinate:[10]

$$G(X) = \left(\frac{1}{\pi\xi^2}\right)^{1/4} e^{-X^2/2\xi^2} \tag{3}$$

and obtain

$$|j,X_a\rangle = v_0 \sum_{\mathbf{r}_e,\mathbf{r}_h} G(X-X_a) F_j(x_e-x_h,\mathbf{r}_{e\perp}-\mathbf{r}_{j\perp};\mathbf{r}_{h\perp} - \mathbf{r}_{j\perp}) a^\dagger_{c\mathbf{r}_e} a_{v\mathbf{r}_h}|0\rangle \tag{4}$$

for the wave function localized at $X=X_a$ with a localization radius ξ. It follows from Eqs. (1) and (4) that

$$\langle j,K|j',X_a\rangle = \delta_{j,j'}(4\pi\xi^2/L^2)^{1/4} e^{-\xi^2K^2/2} e^{-iKX_a} \tag{5}$$

in view of Eq. (2). Note from Eq. (5) that transitions from the localized state to plane-wave state are restricted by the momentum uncertainty condition $K\lesssim\xi^{-1}$.

For Stokes transitions, a direct resonant transition between the same sublevel from the nQWR state $|1,K\rangle$ to the wQWR state $|2,K\rangle$ at a much lower energy is not allowed because energy and momentum cannot be conserved simultaneously. On the other hand, phonon-assisted transition via phonon emission is very slow.[3] The most efficient mechanism in this case is the process whereby the exciton in the initial well breaks up into a free e-h pair in the final well, releasing the extra energy into the kinetic energy $\varepsilon_k \equiv \hbar^2k^2/2\mu$ of the e-h relative motion while conserving the momentum K for the CM motion, where $K=k_e+k_h$, $k=\alpha_e k_h - \alpha_h k_e$, and μ is the reduced mass. The free e-h pair state

consists of the product of the plane-wave states with k_e and k_h:

$$|j,K,k\rangle = \frac{v_0}{L}\sum_{\mathbf{r}_e,\mathbf{r}_h} e^{iKX}e^{-ikx}\phi_e(\mathbf{r}_{e\perp}-\mathbf{r}_{j\perp})\phi_h(\mathbf{r}_{h\perp} - \mathbf{r}_{j\perp})a^{\dagger}_{c\mathbf{r}_e}a_{v\mathbf{r}_h}|0\rangle, \quad (6)$$

where $\phi_e(\mathbf{r}_{e\perp})$ and $\phi_h(\mathbf{r}_{h\perp})$ are the confinement wave functions in the wQWR. Note that the total kinetic energy of this state along the wire can be split into the CM and relative motion: $\hbar^2k_e^2/2m_e+\hbar^2k_h^2/2m_h=E_K+\varepsilon_k$, where $E_K \equiv \hbar^2K^2/2M$ is the CM kinetic energy and is conserved through the transition. In the wQWR, there may be many densely spaced sublevels and one of the high-energy sublevels may be resonant with the ground sublevel of the nQWR as mentioned earlier. In this case, direct resonant transition is important as will be shown later.

III. EXCITON TRANSFER MECHANISM

We consider two exciton transfer mechanisms in this section. One is the standard dipole-dipole interaction and the other is the photon-exchange mechanism mentioned in the Introduction. Defining the dipolar interaction as[7,11]

$$C(x,\mathbf{R}_\perp) = \frac{e^2}{\kappa R^3}[\mathbf{D}_1\cdot\mathbf{D}_2 - 3(\mathbf{R}\cdot\mathbf{D}_1)(\mathbf{R}\cdot\mathbf{D}_2)/R^2], \quad (7)$$

the matrix element for the dipolar coupling between the wires is given by[3]

$$\langle 2,K'|H_{dip}|1,K\rangle = \delta_{K,K'}\int d^2r_\perp \int d^2r'_\perp C(K,\mathbf{R}_\perp)F_2^*(0,\mathbf{r}'_\perp;\mathbf{r}'_\perp) \times F_1(0,\mathbf{r}_\perp;\mathbf{r}_\perp), \quad (8)$$

where $\mathbf{r}_\perp=(y,z)$, $\mathbf{r}'_\perp=(y',z')$, $\mathbf{R}_\perp=(y'-y,z'+d-z)$ is the 2D relative position vector perpendicular to the wire, and $C(K,\mathbf{R}_\perp)=\int\exp(iKx)C(x,\mathbf{R}_\perp)dx$. In Eq. (7), $\mathbf{R}=(x,\mathbf{R}_\perp)$, $R=|\mathbf{R}|$, $\mathbf{D}_j$ is the transition dipole moment, and κ is the bulk dielectric constant. The quantity $C(K,\mathbf{R}_\perp)$ is obtained from Eq. (7) and equals

$$C(K,\mathbf{R}_\perp) = \frac{2e^2}{\kappa R_\perp^2}\{[\mathbf{D}_1\cdot\mathbf{D}_2 - D_{1x}D_{2x} - 2(\hat{\mathbf{R}}_\perp\cdot\mathbf{D}_1) \times(\hat{\mathbf{R}}_\perp\cdot\mathbf{D}_2)]\tilde{K}K_1(\tilde{K}) + [(\hat{\mathbf{R}}_\perp\cdot\mathbf{D}_1)(\hat{\mathbf{R}}_\perp\cdot\mathbf{D}_2) - D_{1x}D_{2x}]\tilde{K}^2K_0(\tilde{K}) - i(D_{2x}\hat{\mathbf{R}}_\perp\cdot\mathbf{D}_1 + D_{1x}\hat{\mathbf{R}}_\perp\cdot\mathbf{D}_2)\tilde{K}^2K_1(\tilde{K})\}, \quad (9)$$

where $R_\perp=|\mathbf{R}_\perp|$, $\hat{\mathbf{R}}_\perp=\mathbf{R}_\perp/R_\perp$, $\tilde{K}=KR_\perp$, and $K_n(x)$ is the nth-order modified Bessel function.

The matrix element for transition from a localized exciton state in the nQWR to a plane-wave state in the wQWR is given in view of Eqs. (5) and (8) by

$$\langle 2,K'|H_{dip}|1,X_a\rangle = (4\pi\xi^2/L^2)^{1/4}\exp(-\xi^2K'^2/2)e^{-iK'X_a} \times\int d^2r_\perp\int d^2r'_\perp C(K',\mathbf{R}_\perp)F_2^*(0,\mathbf{r}'_\perp;\mathbf{r}'_\perp)F_1(0,\mathbf{r}_\perp;\mathbf{r}_\perp). \quad (10)$$

The matrix element for the decay of the exciton in the nQWR into an e-h pair in the wQWR is obtained similarly, yielding

$$\langle 2,K',k'|H_{dip}|1,K\rangle = \frac{\delta_{K,K'}}{\sqrt{L}}\int d^2r_\perp\int d^2r'_\perp C(K,\mathbf{R}_\perp) \times\phi_{2eh\perp}(\mathbf{r}'_\perp)^*F_1(0,\mathbf{r}_\perp;\mathbf{r}_\perp), \quad (11)$$

where $\phi_{jeh\perp}(\mathbf{r}_\perp)=\phi_{je}(\mathbf{r}_\perp)\phi_{jh}(\mathbf{r}_\perp)$ and $\phi_{j\sigma}(\mathbf{r}_\perp)$ is the confinement wave function. We also find

$$\langle 2,K',k'|H_{dip}|1,X_a\rangle = (4\pi\xi^2/L^4)^{1/4}\exp(-\xi^2K'^2/2)e^{-iK'X_a} \times\int d^2r_\perp\int d^2r'_\perp C(K',\mathbf{R}_\perp)\phi_{2eh\perp}(\mathbf{r}'_\perp)^*F_1(0,\mathbf{r}_\perp;\mathbf{r}_\perp). \quad (12)$$

Another coupling mechanism for the exciton transition is through photon exchange. For interwell transfer between two 2D QWs, this mechanism was found to play a major role except for a short distance.[3] In this paper, we assess the relative importance of the photon-exchange transfer in 1D QWRs. The coupling is achieved via two-step processes whereby the electron recombines with the hole in the nQWR emitting a resonant or a virtual photon which travels to the wQWR and excite a valence electron into the conduction band. The final e-h state in w QWR can be an exciton state or a free e-h pair state. In the latter case, the e-h pair forms an exciton rapidly within a time much shorter than the radiative lifetime of the exciton.

The matrix element for the photon-exchange transfer of an exciton in the nQWR into an e-h pair in the wQWR can be calculated following the method given in Ref. 3 and is given for a plane-wave exciton by

$$\langle 2,K',k'|H_{phot-ex}|1,K\rangle = \frac{(eE_gD)^2n}{2\pi\hbar\, c\sqrt{L}}Q(K')\,\delta_{K,K'}, \quad (13)$$

and a localized exciton by

$$\langle 2,K',k'|H_{phot-ex}|1,X_a\rangle = (4\pi\xi^2)^{1/4}\frac{(eE_gD)^2n}{2\pi\hbar\, cL}e^{-iK'X_a} \times\exp(-\xi^2K'^2/2)Q(K'), \quad (14)$$

where

$$Q(K') = \int \delta(K'-q_x)\frac{e^{i(q_zd+q_yy)}P(\mathbf{q})\mathcal{F}_1(\mathbf{q}_\perp)\Phi_{2eh\perp}(\mathbf{q}_\perp)^*}{q(E_g-\hbar\,\omega_q-i\gamma)}d^3q, \quad (15)$$

$$\mathcal{F}_j(\mathbf{q}_\perp) = \int\int \exp(-i\mathbf{q}_\perp\cdot\mathbf{r}_\perp)F_j(0,\mathbf{r}_\perp,\mathbf{r}_\perp)d^2r_\perp, \quad (16)$$

$$\Phi_{jeh\perp}(\mathbf{q}_\perp) = \int\int \exp(-i\mathbf{q}_\perp \cdot \mathbf{r}_\perp)\phi_{jeh\perp}(\mathbf{r}_\perp)d^2r_\perp, \quad (17)$$

and

$$P(\mathbf{q}) = \sum_\lambda [\hat{\mathbf{e}}_\lambda(\mathbf{q}) \cdot \hat{\mathbf{D}}_1][\hat{\mathbf{e}}_\lambda(\mathbf{q}) \cdot \hat{\mathbf{D}}_2]. \quad (18)$$

Here, $\mathbf{q}_\perp = (q_y, q_z)$, $\hat{\mathbf{D}}_j = \mathbf{D}_j/D_j$, $D_j = |\mathbf{D}_j|$, and $\hat{\mathbf{e}}_\lambda(\mathbf{q})$ is the polarization vector for the photon with mode λ, the energy $\hbar\omega_q$, the wave vector $\mathbf{q}$, and γ is a negligibly small damping parameter. In Eqs. (13) and (14), E_g is the band gap and n is the refractive index, while the quantity y in Eq. (15) is the y coordinate of the center of the wQWR relative to that of the nQWR. This notation y is chosen for its simplicity and is not to be confused with the dummy variable y in Eqs. (16) and (17).

Similarly, coupling between plane-wave and localized exciton states in the nQWR and a plane-wave state in the wQWR through photon exchange is given by

$$\langle 2, K'|H_{phot-ex}|1, K\rangle = \frac{(eE_gD)^2 n}{2\pi\hbar c} R(K') \quad (19)$$

and

$$\langle 2, K'|H_{phot-ex}|1, X_a\rangle = (4\pi\xi^2/L^2)^{1/4} \frac{(eE_gD)^2 n}{2\pi\hbar c} e^{-iK'X_a} \times \exp(-\xi^2 K'^2/2) R(K'), \quad (20)$$

respectively. Here,

$$R(K') = \int \delta(K' - q_x) \frac{e^{i(q_z d + q_y y)} P(\mathbf{q}) \mathcal{F}_1(\mathbf{q}_\perp) \mathcal{F}_2(\mathbf{q}_\perp)^*}{q(E_g - \hbar\omega_q - i\gamma)} d^3q. \quad (21)$$

The quantity $P(\mathbf{q})$ can readily be evaluated for the case $\mathbf{D}_1 \| \mathbf{D}_2$, yielding[12]

$$P(\mathbf{q}) = \frac{q_\perp^2}{q^2}, \quad (22)$$

where $q_\perp$ is the component of $\mathbf{q}$ perpendicular to $\mathbf{D}_j$. For the case $\mathbf{D}_1 \perp \mathbf{D}_2$, we find[12]

$$P(\mathbf{q}) = -\frac{(\mathbf{q} \cdot \hat{\mathbf{D}}_1)(\mathbf{q} \cdot \hat{\mathbf{D}}_2)}{q^2}. \quad (23)$$

IV. TRANSITION RATE

We consider exciton transfer from plane-wave states $|1, i\rangle = |1, K\rangle$ or localized states $|1, i\rangle = |1, X_a\rangle$ in the ground sublevel of the nQWR to final states $|2, f\rangle$ in the wQWR. The analysis presented in this section is applicable to both dipole-dipole and photon-exchange energy transfer. Defining E_{12} as the difference between the sum of the electron and hole sublevel energies of the initial and the final QWRs as illustrated in the bottom inset of Fig. 1, E_{12} is large for transitions between the ground sublevels in typical asymmetric QWRs. In this case, inelastic processes are required to dissipate the extra energy in the nQWR. It turns out that phonon-assisted processes are not efficient.[3] The extra energy is more efficiently dissipated through creation of free e-h pairs in the wQWR.[1,3] This rate equals

$$W_{eh} = \frac{2\pi}{\hbar} \left\langle \sum_{K',k'} |\langle 2, K', k'|H|1, i\rangle|^2 \delta(E_i + E_{12}^* - E_{K'} - \varepsilon_{k'}) \right\rangle_{av}, \quad (24)$$

where the matrix elements are given by Eqs. (11)–(14), $E_{12}^* = E_{12} - E_{nB}$, E_{nB} is the exciton binding in the nQWR, the triangular brackets signify the thermal average over the initial energy E_i, and $E_i = E_K$ for the plane-wave states. For localized excitons, we assume $E_i = 0$ for the numerical evaluation later and omit thermally averaging over the initial states. The latter is determined by the density of states which, in turn, is determined by the dependence of the exciton energy on ξ and the distribution of ξ. These quantities are not well known.

The k' summation in Eq. (24) can be readily carried out since the matrix element is independent of k', yielding

$$W_{eh} = \frac{\sqrt{2\mu}L}{\hbar^2} \left\langle \sum_{K'} \frac{|\langle 2, K', k'|H|1, i\rangle|^2}{\sqrt{E_i + E_{12}^* - E_{K'}}} \theta(E_i + E_{12}^* - E_{K'}) \right\rangle_{av}, \quad (25)$$

where $\theta(x)$ is a unit step function. Here, k' is maintained in the notation for the matrix element $\langle 2, K', k'|H|1, i\rangle$ to indicate the nature of the final state, although it is independent of k'. For the plane-wave states $i = K$, Eq. (25) yields, in view of $K = K'$,

$$W_{eh} = \frac{2\sqrt{2\mu}L}{\hbar^2 K_T \sqrt{\pi}} \frac{\theta(E_{12}^*)}{\sqrt{E_{12}^*}} \int_0^\infty \exp[-(K/K_T)^2] \times |\langle 2, K, k'|H|1, K\rangle|^2 dK, \quad (26)$$

where $K_T = \sqrt{2Mk_BT}/\hbar$ is basically the cutoff wave number and T is the temperature. For localized states we use Eqs. (11) and (12) and find

$$W_{eh} = \frac{2\sqrt{2\mu}L}{\hbar^2 K_\xi \sqrt{\pi}} \int_0^\infty \exp[-(K/K_\xi)^2] \times |\langle 2, K, k'|H|1, K\rangle|^2 \frac{\theta(E_i + E_{12}^* - E_K)}{\sqrt{E_i + E_{12}^* - E_K}} dK. \quad (27)$$

Here, the K integration [i.e., the K' summation in Eq. (25)] extends effectively to the cuttoff wave number $K_\xi \equiv 1/\xi$. Note that the dependence of W_{eh} on K_T in Eq. (26) is the same as the dependence of W_{eh} on K_ξ in Eq. (27) in the limit of large ξ, where E_{K_ξ} is negligibly small in the denominator of Eq. (27). Namely, the ξ dependence of W_{eh} in Eq. (27) can be obtained from the T dependence of W_{eh} in Eq. (26) and vice versa through the interchange $T \leftrightarrow k_B^{-1}\hbar^2\xi^{-2}/2M$ or equivalently $\xi/\text{Å} \leftrightarrow 2.103 \times 10^2 \sqrt{m_o/MT}$, where T is in K.

If the final state is in the excited sublevel in wQWR which is nearly resonant with the ground sublevel of the nQWR, a direct resonant transfer into final exciton states is very efficient. The transfer rate is given by[3]

$$W_{res} = \frac{2}{\hbar}\left\langle \sum_{K'} \frac{|\langle 2,K'|H|1,i\rangle|^2 \Gamma_{2K'}(E_{1i})}{(E_i + E_{12}^{**} - E_{K'})^2 + \Gamma_{2K'}(E_{1i})^2} \right\rangle_{av}, \quad (28)$$

where $E_{12}^{**} = E_{12} - E_{nB} + E_{wB}$ is the net energy mismatch and $\Gamma_{2K'}(E_{1i})$ is damping in the wQWR at the initial total energy $E_{1i} \equiv E_1 - E_{nB} + E_i$. Here, E_1 (E_2) is the sum of the electron and hole sublevel energies in the nQWR (wQWR). The matrix element $\langle 2,K'|H|1,i\rangle$ is given by Eqs. (8), (10), (19), and (20). In Eq. (28), we neglect damping in the ground state of the nQWR compared with that of the excited state of the wQWR.

For plane-wave states $|1,i\rangle = |1,K\rangle$ with $E_i = E_K$, Eq. (28) equals

$$W_{res} = \frac{4}{\hbar K_T \sqrt{\pi}} \int_0^\infty \exp[-(K/K_T)^2]\theta(E_{12}^{**} + E_K) \frac{|\langle 2,K|H|1,K\rangle|^2 \Gamma_{2K}(E_{1i})}{E_{12}^{**2} + \Gamma_{2K}(E_{1i})^2} dK, \quad (29)$$

where $E_{1i} = E_1 - E_{nB} + E_K$. For localized states, Eq. (28) yields

$$W_{res} = \frac{2\sqrt{2\pi M}\,\theta(E_{12}^{**} + E_i)}{\hbar^2 K_\xi \sqrt{E_K}} \exp[-(K/K_\xi)^2] \times |\langle 2,K|H|1,K\rangle|^2 \Big|_{E_K = E_{12}^{**} + E_i}. \quad (30)$$

If the initial energy E_{1i} is below the band bottom $E_{2f} = E_2 - E_{wB}$ of the final energy of the wQWR (corresponding to anti-Stokes transfer), the quantity $\Gamma_{2K}(E_{1i})$ and therefore W_{res} vanishes as indicated by the unit step functions in Eqs. (29) and (30), requiring an activated energy E_i, yielding small W_{res} at low temperatures. On the other hand, the matrix element becomes small, $|\langle 2,K|H|1,K\rangle| \propto \exp(-\tilde{K}) \ll 1$, for $\tilde{K} \gg 1$ if E_{1i} is too far above E_{2f}. There is an additional Gaussian cutoff factor K_T for the plane-wave states and K_ξ for the localized states.

V. APPROXIMATIONS

In this section, we introduce approximations in order to simplify the numerical evaluation for an order of magnitude estimate of the transfer rate. These approximations can be improved for a better accuracy but with a longer computation time. The exciton wave function is determined by the electron hole (e-h) Coulomb attraction potential and the confinement energy of the electron and the hole in the perpendicular directions and cannot be solved exactly. We therefore make the following approximation

$$F_j(x, \mathbf{r}_{e\perp}, \mathbf{r}_{h\perp}) = \psi_j(x)\phi_{je}(\mathbf{r}_{e\perp})\phi_{jh}(\mathbf{r}_{h\perp}), \quad (31)$$

where $\phi_\sigma(\mathbf{r}_{\sigma\perp})$ is the confinement wave function in a given y sublevel in the absence of e-h interaction and $\psi(x)$ is determined by

$$\left(-\frac{\hbar^2}{2\mu}\frac{d^2}{dx^2} + V_{jeh}(x)\right)\psi_j(x) = E\psi_j(x), \quad (32)$$

where μ is the reduced mass and $V_{jeh}(x)$ is the effective e-h attraction given by[9]

$$V_{jeh}(x) = -\frac{e^2}{\kappa}\int d^2 r_{e\perp} \int d^2 r_{h\perp} \frac{|\phi_{je}(\mathbf{r}_{e\perp})\phi_{jh}(\mathbf{r}_{h\perp})|^2}{\sqrt{x^2 + (\mathbf{r}_{e\perp} - \mathbf{r}_{h\perp})^2}}. \quad (33)$$

The eigenfunction $\psi_j(x)$ is obtained numerically.

We also assume that the size of the cross sections of the wires is small compared with the interwire distance d and ξ_g defined by $\hbar\omega_g \equiv E_g$ with $q = \xi^{-1}$. For GaAs QWRs, we estimate $\xi_g = 353$ Å for $E_g = 1.52$ eV and $n = 3.68$. These approximations yield $\mathbf{R}_\perp = (0,y,d)$, $R_\perp = r \equiv \sqrt{d^2 + y^2}$, and $\tilde{K} = Kr$, where y was defined earlier for $Q(K)$ in Eq. (15). Equation (9) then reduces to

$$C(K,r) \equiv \frac{2e^2}{\kappa r^2}[(D_{1y}D_{2y} - D_{1z}D_{2z})\tilde{K}K_1(\tilde{K}) + (D_{1z}D_{2z} - D_{1x}D_{2x})\tilde{K}^2 K_0(\tilde{K}) - i(D_{1z}D_{2x} + D_{1x}D_{2z})\tilde{K}^2 K_1(\tilde{K})]. \quad (34)$$

We can also simplify Eqs. (8) and (10)–(12) to

$$\langle 2,K'|H_{dip}|1,K\rangle = \delta_{K,K'} C(K,r)\psi_1(0)\psi_2^*(0)\Phi_{1eh\perp}(0)\Phi_{2eh\perp}(0)^*, \quad (35)$$

$$\langle 2,K'|H_{dip}|1,X_a\rangle = (4\pi\xi^2/L^2)^{1/4}\exp(-\xi^2 K'^2/2)e^{-iK'X_a} \times C(K',r)\psi_1(0)\psi_2^*(0)\Phi_{1eh\perp}(0)\Phi_{2eh\perp}(0)^*, \quad (36)$$

$$\langle 2,K',k'|H_{dip}|1,K\rangle = \frac{\delta_{K,K'}}{\sqrt{L}} C(K,r)\psi_1(0)\Phi_{1eh\perp}(0)\Phi_{2eh\perp}(0)^*, \quad (37)$$

and

$$\langle 2,K',k'|H_{dip}|1,X_a\rangle = (4\pi\xi^2/L^4)^{1/4}\exp(-\xi^2 K'^2/2)e^{-iK'X_a} \times C(K',r)\psi_1(0)\Phi_{1eh\perp}(0)\Phi_{2eh\perp}(0)^*, \quad (38)$$

respectively, in view of Eq. (17). In Eq. (38), $\Phi_{jeh\perp}(0) = 1$ for an infinitely deep square-well potential or if the difference between the electron and the hole confinement wave functions are ignored in the wQWR.

Similarly, we also find, for the photon-exchange interaction,

$$Q(K) = \psi_1(0)\Phi_{1eh\perp}(0)\Phi_{2eh\perp}(0)^* S(K) \quad (39)$$

for Eqs. (13) and (14) and

$$R(K) = \psi_1(0)\psi_2(0)\Phi_{1eh\perp}(0)\Phi_{2eh\perp}(0)^* S(K) \quad (40)$$

for Eqs. (19) and (20), where

$$S(K) = \int \delta(K - q_x) \frac{e^{i(q_z d + q_y y)} P(\mathbf{q})}{q(E_g - \hbar\omega_q - i\gamma)} d^3q. \tag{41}$$

Designating $S(K)$ as $S_{uv}(K)$ for the case $\mathbf{D}_1 \| \mathbf{u}$ and $\mathbf{D}_2 \| \mathbf{v}$ in Eq. (18) where $\mathbf{u}$ and $\mathbf{v}$ are unit vectors which can lie in any of the x, y, and z directions, the following useful identities are obtained from Eqs. (22), (23), and (41):

$$S_{xx}(K) = 2\pi \int_0^\infty \frac{J_0(q_\perp r) q_\perp^3 dq_\perp}{q^3(E_g - \hbar\omega_q - i\gamma)}, \tag{42}$$

$$S_{yy}(K) = 2\pi \int_0^\infty \frac{[(q^2 - q_\perp^2 y^2/r^2) J_0(q_\perp r) + q_\perp (r^2 - 2y^2) J_0'(q_\perp r)/r^3] q_\perp dq_\perp}{q^3(E_g - \hbar\omega_q - i\gamma)}, \tag{43}$$

and

$$S_{zz}(K) = 2\pi \int_0^\infty \frac{[(K^2 + y^2 q_\perp^2/r^2) J_0(q_\perp r) + q_\perp (2y^2 - r^2) J_0'(q_\perp r)/r^3] q_\perp dq_\perp}{q^3(E_g - \hbar\omega_q - i\gamma)}, \tag{44}$$

where $q = \sqrt{K^2 + q_\perp^2}$, $J_0(x)$ is the zeroth-order Bessel function, and use is made of the relationship $xJ_0''(x) = -[J_0'(x) + xJ_0(x)]$. Here, the prime means the derivative with respect to the argument. We also find

$$(S_{xy}(K), S_{xz}(K)) = 2\pi i K \frac{(y,d)}{r} \int_0^\infty \frac{J_0'(q_\perp r) q_\perp^2 dq_\perp}{q^3(E_g - \hbar\omega_q - i\gamma)} \tag{45}$$

and

$$S_{yz}(K) = -\frac{2\pi y d}{r^3} \int_0^\infty \frac{[r q_\perp J_0(q_\perp r) + 2J_0'(q_\perp r)] q_\perp^2 dq_\perp}{q^3(E_g - \hbar\omega_q - i\gamma)}. \tag{46}$$

VI. NUMERICAL EVALUATIONS AND DISCUSSIONS

We assume harmonic potentials for the confinement wave functions $\phi_\sigma(\mathbf{r}_{\sigma\perp})$. The Hamiltonian in Eq. (32) for motion in the $s = y, z$ direction is given by

$$H_\sigma = \frac{\hbar\omega_\sigma}{2} \left(-\frac{\partial^2}{\partial \tilde{s}^2} + \tilde{s}^2 \right), \tag{47}$$

where $\tilde{s} = s/\ell_\sigma$ is the reduced coordinate and $\ell_\sigma = \sqrt{\hbar/\omega_\sigma m_\sigma}$. The four-dimensional integration in Eq. (33) can be simplified if we assume that the confinement length $\sim \ell_\sigma$ (but not the energy $\hbar\omega_\sigma$) is the same for the electron and the hole and depends only on the direction $\ell_\sigma \equiv \ell_s$. This situation occurs for a deep rectangular potential of width L_s. By equating the ground sublevel energies from the two models, we estimate $\ell_s \sim L_s/\sqrt{\pi}$. This relationship will be used to indicate the approximate size of the cross section of the QWR. For the z direction, only the ground sublevel $n = 0$ is considered while excited levels are allowed in the y direction for possible resonant transfer. It is convenient for the integrations in Eq. (33) to rotate the coordinate into the new axes $z_+ = z_e + z_h$, $z_- = z_e - z_h$, $y_+ = y_e + y_h$, and $y_- = y_e - y_h$. The effective e-h potential is then given, after carrying out the z_+ integration, by

$$V_{eh}(x) = -\frac{e^2}{2\sqrt{2\pi}\kappa\ell_z} \int\int\int \frac{\exp(-z_-^2/2\ell_z^2) \rho_n(y_e) \rho_n(y_h)}{\sqrt{x^2 + z_-^2 + y_-^2}} dz_- dy_+ dy_-, \tag{48}$$

where $n = 0, 1, 2, \ldots$ and

$$\rho_n(y) = \frac{1}{2^n n!\, \ell \sqrt{\pi}} \exp(-y^2/\ell_y^2) H_n(y/\ell_y)^2. \tag{49}$$

Here, $H_n(x)$ is the nth-order Hermite polynomial. The y_+ integration can be carried out for $n = 0$ using $y_e^2 + y_h^2 = (y_+^2 + y_-^2)/2$ in the exponent of the the product $\rho_n(y_e)\rho_n(y_h)$. For $n > 0$, the product contains a polynomial of powers of y_+ and y_-. The y_+ integration can be carried out analytically term by term, leaving only the z_- and y_- integrations, which are carried out numerically.

For a numerical evaluation, we use for GaAs QWRs (Ref. 3) $\kappa = 12.4$, $D_1 = D_2 = 5.5$ Å, $m_e = 0.067 m_0$ where m_0 is the free electron mass and $m_h = 0.16 m_0$.[13] The $n = 0$ binding energies are given by 14.5 and 10.1 meV, respectively, for $L_z = 5$, $L_y = 10$ nm assumed for the nQWR and $L_z = 8$, $L_y = 16$ nm assumed for the wQWR.[5] For the level $n = 2$ of the wQWR, we find 6.0 meV for the binding energy. Initially, we study transfer to a single wQWR at $y = 0$ at a distance $r = d$. The effect of the energy transfer to a planar array of parallel wQWRs will be discussed later.

Figure 2 displays the dipole-dipole transfer rate W_{eh} in Eq. (26) for an effective energy mismatch $E_{12}^* = 22.6$ meV. In general, the dipole moments are given by a linear combination of the components in the x, y, and the z directions. For the purpose of order of the magnitude estimate, we consider the following three cases. The dashed, solid, and dashed-dotted curves correspond, respectively, to the cases where $\mathbf{D}_1$ and $\mathbf{D}_2$ are (i) both in the x axis, (ii) randomly in the x, y axes, and (iii) in the x, y, z directions. The top dashed-dotted curve is roughly parallel to $1/d^4$ in the range $d < 180$ Å. The

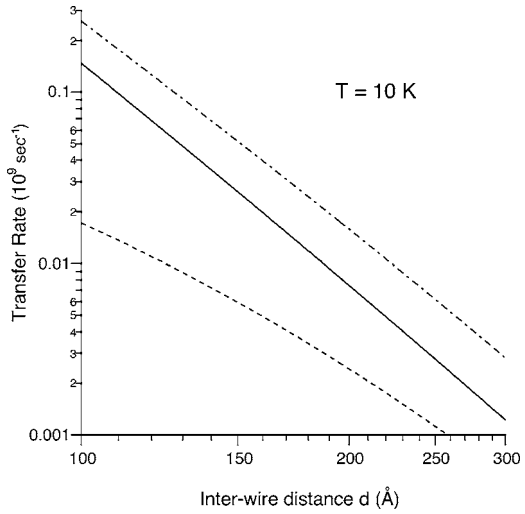

FIG. 2. Dipole-dipole transfer rates (between two bold QWRs in Fig. 1 with $y=0$) of plane-wave excitons through electron-hole pair creation at 10 K as a function of the center-to-center distance d for an effective energy mismatch $E_{12}^{*}=E_{12}-E_{nB}=22.6$ meV. The dipole moments lie in the x (wire) direction for the dashed curve, in the x, y directions for the solid curve, and in the x, y, z directions for the dashed-dotted curve. Other parameters are given in the text.

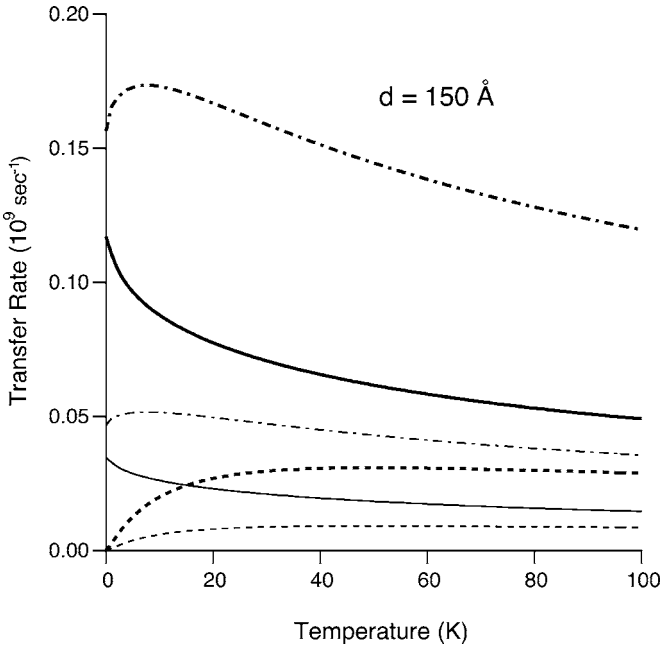

FIG. 3. The temperature dependence of the transfer rate studied in Fig. 2 for an effective energy mismatch $E_{12}^{*}=E_{12}-E_{nB}=22.6$ meV (thin curves) at a center-to-center distance $d=150$ Å. The dipole moments lie in the x (wire) direction for the dashed curve, in the x, y directions for the solid curve, and in the x, y, z directions for the dashed-dotted curve. Other parameters are given in the text. The thick curves show enhanced rates for a small effective energy mismatch $E_{12}^{*}=E_{12}-E_{nB}=2$ meV.

asymptotic rate follows $1/d^4$ or $1/d^5$depending on the temperature. The asymptotic behavior originates from the $\tilde{K}$-dependence of Eq. (34). Defining $d_T=1/K_T$, the rate in Eq. (26) is proportional to

$$W_{eh} \propto \frac{1}{r^5}\int_0^\infty \exp[-(d_T/r)^2\tilde{K}^2]f(\tilde{K})^2 d\tilde{K},$$

where $f(\tilde{K})$ is the the quantity inside the square brackets of Eq. (34), namely $f(\tilde{K})=\kappa r^2 C(K,r)/2e^2$. For $d_T \ll r$, the main contribution to the integral arises from $\tilde{K} \lesssim 1$ in view of $K_n(x) \to e^{-x}\sqrt{\pi/2x}$ for $x \gg 1$ and becomes independent of r, yielding $W_{eh} \propto 1/r^5 = 1/d^5$ for $y=0$ for all the curves in Fig. 2. This d dependence is expected from a crude dimensional analysis showing that the dipole-dipole rate has a $R^{-6}=(x^2+y^2+d^2)^{-3}$ dependence according to Eq. (7). Integrating this quantity over $-\infty < x < \infty$ for $y=0$ yields the above d^{-5} dependence. For transfer to a 2D QW or a planar array of parallel the wQWRs, another integration over $-\infty < y < \infty$ yields a d^{-4} dependence. For $d_T \gg r$ on the other hand, the main contribution arises from $\tilde{K} \lesssim r/d_T \ll 1$, where $f(\tilde{K})$ is independent of $\tilde{K}$ for cases 2 and 3 above, yielding $W_{eh} \propto 1/r^4 = 1/d^4$ for the solid and dashed-dotted curves in Fig. 2. For the dashed curve, a similar analysis shows that W_{eh} has a much slower d dependence. We find $d_T=140$ Å at 10 K: The curves are entering the asymptotic limit $W_{eh} \propto 1/d^5$near the upper range of d in Fig. 2.

The three thin curves in Fig. 3 show the temperature dependence of the rates studied in Fig. 2 at a distance $d=150$ Å. The thick curves show enhanced rates for a much smaller effective energy mismatch $E_{12}^{*}=E_{12}-E_{nB}=2$ meV for the same parameters otherwise. In this case, the energy dissipated into the relative e-h motion is small, yielding a larger rate due to the enhanced 1D density of states (with a van Hove singularity) at a low energy.

Figure 4 displays the dipole-dipole transfer rates W_{eh} of the localized excitons in Eq. (27) for $\xi=60$ Å (thin curves) and $\xi=200$ Å (thick curves) for $E_{12}^{*}=E_{12}-E_{nB}=22.6$ meV. As discussed earlier, the ξ dependence of the rate here can be deduced from the T dependence of the rate obtained in Eq. (26) and studied in Fig. 3 through the fact that the K_T dependence of the latter is the same as the K_ξ $(=1/\xi)$ dependence of the former for large ξ. This property is shown more clearly in the next figure.

Figure 5 shows the dipole-dipole transfer rates W_{eh} of the localized excitons in Eq. (27) as a function of ξ for $d=100$ Å (thin curves) and $d=150$ Å (thick curves) for $E_{12}^{*}=E_{12}-E_{nB}=22.6$ meV for comparison with the temperature dependence of W_{eh}. The near saturation for the upper four curves above $\xi > 300$ Å is correlated with the saturation of the upper four curves in Fig. 3 below 1 K as discussed in Sec. IV following Eq. (27). Similarly, the continuous decrease of the other two lower dashed curves below ~30 K in Fig. 3 is correlated with the continuous decrease of the two dashed curves above $\xi > 50$ Å in Fig. 5.

Figure 6 displays resonant dipole-dipole transfer rates obtained from Eqs. (29) and (30) for the case where e1h1 energy in the nQWR is nearly resonant with the e3h3 energy in the wQWR with a net energy mismatch $E_{12}^{**}=1$ meV. Here, n_σ for the notation $en_e hn_h$ indicates the sublevel index in the y direction. The rates for localized initial excitons (thick

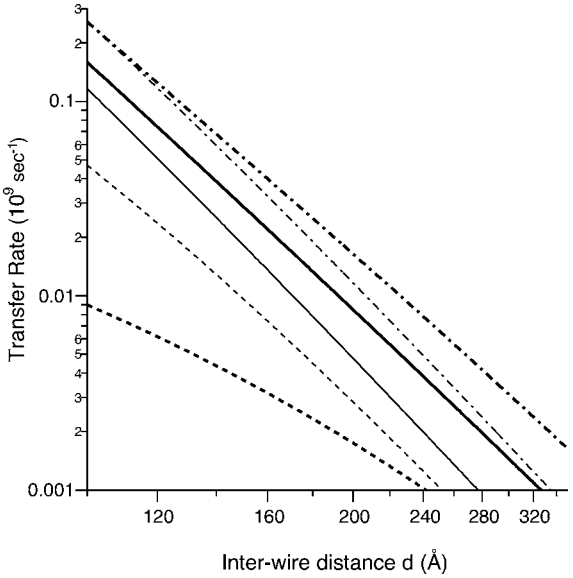

FIG. 4. Dipole-dipole transfer rates of localized excitons through electron-hole pair creation as a function of the center-to-center distance d for $\xi=60$ Å (thin curves) and $\xi=200$ Å (thick curves) for an effective energy mismatch $E_{12}^{*}=E_{12}-E_{nB}=22.6$ meV. The dipole moments lie in the x (wire) direction for the dashed curve, in the x,y directions for the solid curve, and in the x, y, z directions for the dashed-dotted curve. Other parameters are given in the text.

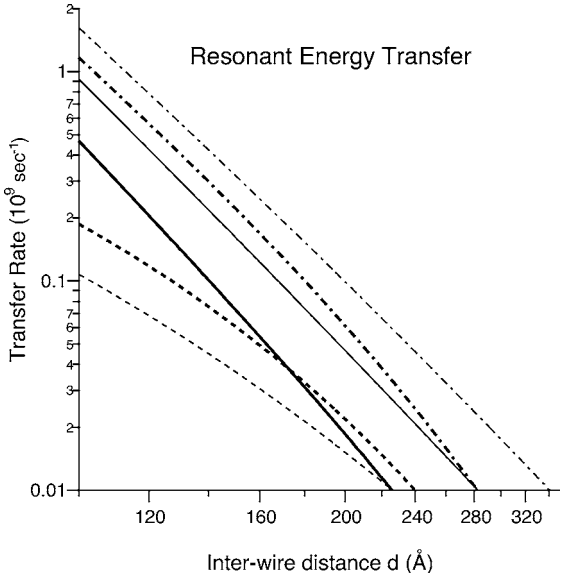

FIG. 6. Resonant dipole-dipole transfer rates from e1h1 exciton state of the nQWR to plane-wave states of e3h3 exciton of the wQWR for a net energy mismatch $E_{12}^{**}=E_{12}-E_{nB}+E_{wB}=1$ meV for $\xi=60$ Å (localized initial excitons: thick curves) and for $T=10$ K and $\Gamma=1$ meV (plane-wave initial excitons: thin curves). The dipole moments lie in the x (wire) direction for the dashed curve, in the x, y directions for the solid curve, and in the x, y, z directions for the dashed-dotted curve. Other parameters are given in the text.

curves) are for $\xi=60$ Å, while $T=10$ K and $\Gamma=1$ meV for the plane-wave states (thin curves). The enhancement of the transfer rate W_{eh} via creation of e-h pairs for the nearly resonant case was discussed earlier for the thick curves in Fig. 3.

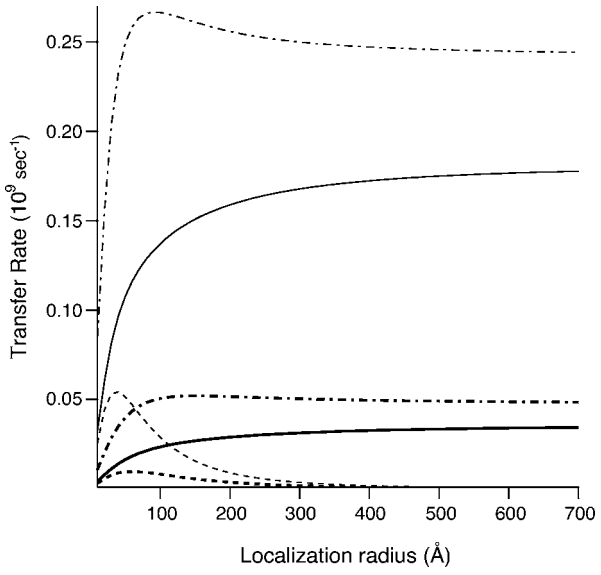

FIG. 5. Dipole-dipole transfer rates of localized excitons through electron-hole pair creation as a function of the localization radius ξ for $d=100$ Å (thin curves) and $d=200$ Å (thick curves) for an effective energy mismatch $E_{12}^{*}=E_{12}-E_{nB}=22.6$ meV. The dipole moments lie in the x (wire) direction for the dashed curve, in the x, y directions for the solid curve, and in the x, y, z directions for the dashed-dotted curve. Other parameters are given in the text.

The four curves in Fig. 7 show the photon-exchange transfer rate W_{eh} in Eq. (27) of localized excitons with $\xi=60$ Å for an effective energy mismatch $E_{12}^{*}=22.6$ meV for $\mathbf{D}_1\|\mathbf{D}_2\|\mathbf{x}$ (dashed curve), $\mathbf{D}_1\|\mathbf{D}_2\|\mathbf{y}$ (solid curve), $\mathbf{D}_1\|\mathbf{D}_2\|\mathbf{z}$ (dashed-dotted curve), and $\mathbf{D}_1\|\mathbf{x};\mathbf{D}_2\|\mathbf{z}$ (dotted curve). The rates decrease very slowly with d. For example, the dotted

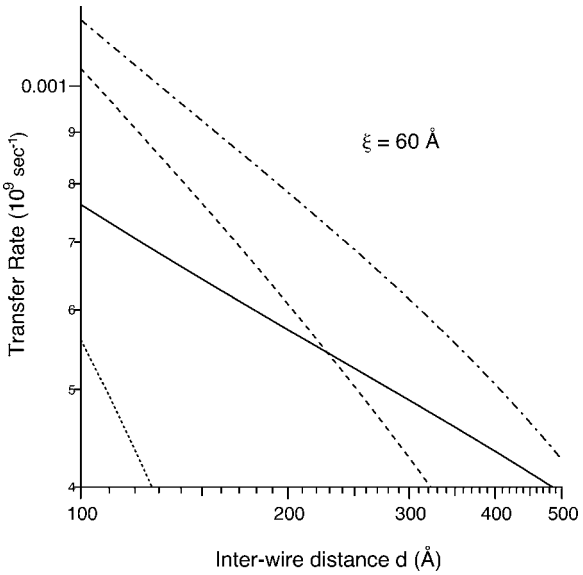

FIG. 7. The photon-exchange transfer rate of localized excitons through electron-hole pair creation from the nQWR to the wQWR for $E_{12}^{*}=22.6$ meV, $\xi=60$ Å, and $\mathbf{D}_1\|\mathbf{D}_2\|\mathbf{x}$ (dashed curve), $\mathbf{D}_1\|\mathbf{D}_2\|\mathbf{y}$ (solid curve), $\mathbf{D}_1\|\mathbf{D}_2\|\mathbf{z}$ (dashed-dotted curve), and $\mathbf{D}_1\|\mathbf{x};\ \mathbf{D}_2\|\mathbf{z}$ (dotted curve).

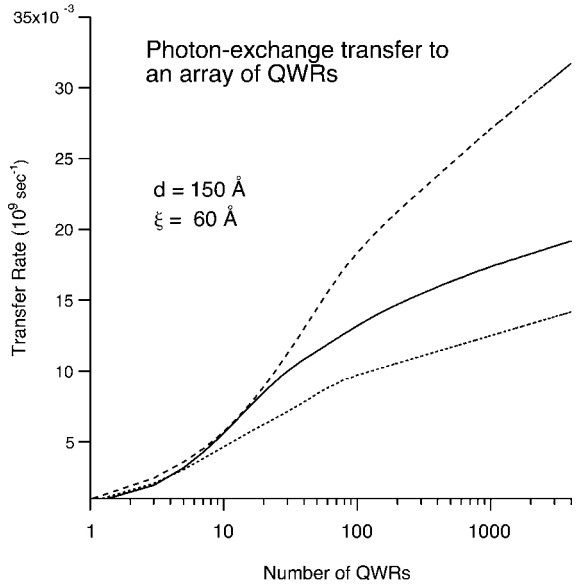

FIG. 8. The total photon-exchange transfer rate of localized excitons through electron-hole pair creation from the nQWR to a uniform array of N_w parallel wQWRs at a perpendicular distance d =150 Å as a function of N_w for E_{12}^{*}=22.6 meV, ξ=60 Å, and $\mathbf{D}_1\|\mathbf{D}_2\|\mathbf{x}$ (dotted curve), $\mathbf{D}_1\|\mathbf{D}_2\|\mathbf{y}$ (solid curve), and $\mathbf{D}_1\|\mathbf{D}_2\|\mathbf{z}$ (dashed curve). The center-to-center separation of the w QWRs is 100 Å.

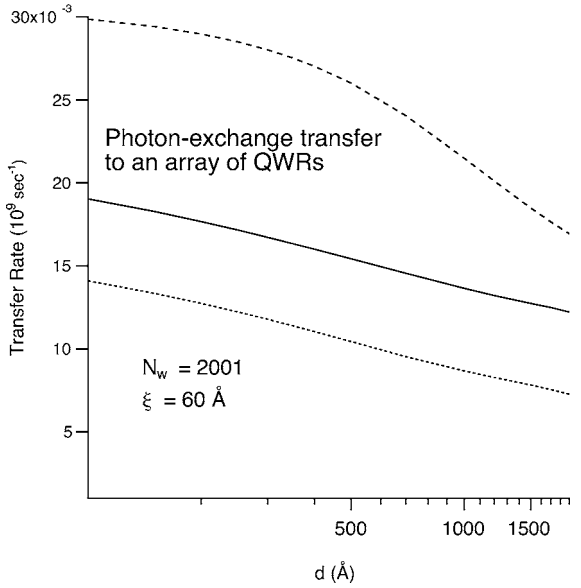

FIG. 9. The total photon-exchange transfer rate of localized excitons through electron-hole pair creation from the nQWR to a uniform array of N_w=2001 parallel wQWRs as a function of the perpendicular distance d for E_{12}^{*}=22.6 meV, ξ=60 Å, and $\mathbf{D}_1\|\mathbf{D}_2\|\mathbf{x}$ (dotted curve), $\mathbf{D}_1\|\mathbf{D}_2\|\mathbf{y}$ (solid curve), and $\mathbf{D}_1\|\mathbf{D}_2\|\mathbf{z}$ (dashed curve). The center-to-center separation of the wQWRs is 100 Å.

curve at the bottom is nearly proportional to d^{-1}. Other curves reach this behavior at greater values of d. This dependence on d is expected because the photon-exchange transfer rate between two zero-dimensional systems (i.e., quantum dots) is given by[14] $W \propto R^{-2}=(x^2+y^2+d^2)^{-1}$. Integrating over x yields $W \propto d^{-1}$ for $y=0$. For 2D QWs or a 2D array of QWRs to be studied below, an additional integration over y yields a very slow d dependence: $W \propto \ln(y_o/d)$, where y_o is roughly the sample dimension in the y direction or the photon attenuation length (i.e., mean free path) whichever is the smaller.[3,15] This behavior is demonstrated for a 2D array of wires in Figs. 8 and 9 to be studied below. The resonant photon-exchange transfer rate will not be shown because it is comparatively small. This is due to the fact that even for the small wave number corresponding to the small plane-wave exciton energy of E_{12}^{**}=1 meV, the photon energy is still large, yielding a large intermediate-state energy in the denominator of Eq. (41) and thereby a small rate. This is in contrast with W_{eh} where the denominator can be resonant, yielding a larger rate.

Figure 8 shows the total transition rate from the nQWR to a planar array of parallel wQWRs at a distance d=150 Å as a function of the number N_w of wQWRs for the same parameters employed for Fig. 7. The wQWRs are uniformly separated by a center-to-center distance 100 Å symmetrically with respect to the center QWR at $y=0$ studied in Fig. 7. The dashed, solid, and dotted curves in Figs. 8 and 9 represent the cases $\mathbf{D}_1\|\mathbf{D}_2\|\mathbf{z}$, $\mathbf{D}_1\|\mathbf{D}_2\|\mathbf{y}$, and $\mathbf{D}_1\|\mathbf{D}_2\|\mathbf{x}$, respectively. It is clear from Fig. 8 that the total rate keeps increasing logarithmically, demonstrating the long-range and macroscopic nature of the photon-exchange transfer. Figure 9 shows the slow logarithmic d dependence of the total transition rate for the same array of N_w=2001 wQWRs. It is interesting to note here that the power-law behavior in Fig. 7 for transfer to a single QWR is altered into a logarithmic d dependence, demonstrating the dominant influence of the distant QWRs in the array and the macroscopic nature of the photon-exchange transfer. The results demonstrated above for the array are consistent with the earlier predictions of the results for 2D-2D transfer.[3]

In contrast with the above behavior of photon-exchange energy transfer, the transfer rate through dipolar interaction saturates very quickly with the array size as shown in Fig. 10 for free excitons (a) and localized excitons with ξ=60 Å (b). Here, the perpendicular distance between the nQWR and the array is d=150 Å. Other parameters are the same as given for Fig. 2 and Figs. 4–6. The thick and thin curves represent resonant transfer and transfer via e-h pair creation, respectively. The style of the curves has the same meaning as in Fig. 2. The curves saturate near N_w=11 reflecting the short-ranged nature of the dipolar interaction. Figure 11 displays the total transfer rate through e-h pair creation as a function of the perpendicular distance d for an array of N_w=11 wQWRs for plane wave (thick curves) and localized (thin curves). The rate reaches a d^{-4} dependence for all the curves at $d>500$ Å as anticipated. Note that the dipolar transfer rate here becomes smaller than the photon-exchange transfer rate shown in Fig. 9 at a large distance roughly beyond $d \gtrsim 160-200$ Å. For transfer between 2D GaAs QWs, this crossover occurs at a much shorter distance $d \gtrsim 80$ Å.[3]

Recently, Karlsson *et al.*[5] observed energy transfer between two GaAs V-groove QWRs with thicknesses L_z =5.4 nm (nQWR) and L_z=8.2 nm (wQWR). They found efficient transfer for samples with a center barrier thickness L_b=5.5 nm and L_b=8.5 nm but not for L_b=13 nm and L_b

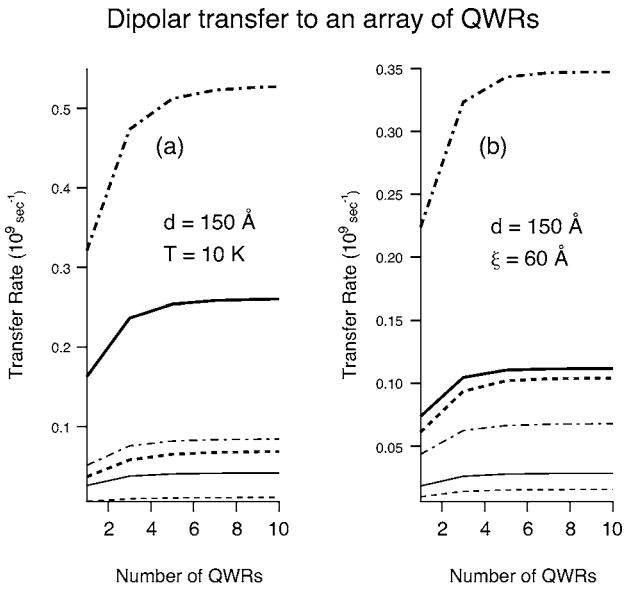

FIG. 10. The total dipolar transfer rate of plane-wave (a) and localized (b) excitons from the nQWR to a uniform symmetric array of N_w parallel wQWRs as a function of N_w for $E_{12}^*=22.6$ meV (thin curves) and $E_{12}^*=\Gamma=1$ meV (thick curves) at a perpendicular distance $d=150$ Å. The center-to-center separation of the wQWRs is 100 Å. The thick curves represent resonant transfer and the thin curves indicate transfer through e-h pair creation. The dipole moments lie in the x (wire) direction for the dashed curve, in the x, y directions for the solid curve, and in the x, y, z directions for the dashed-dotted curve. Other parameters are given in the text.

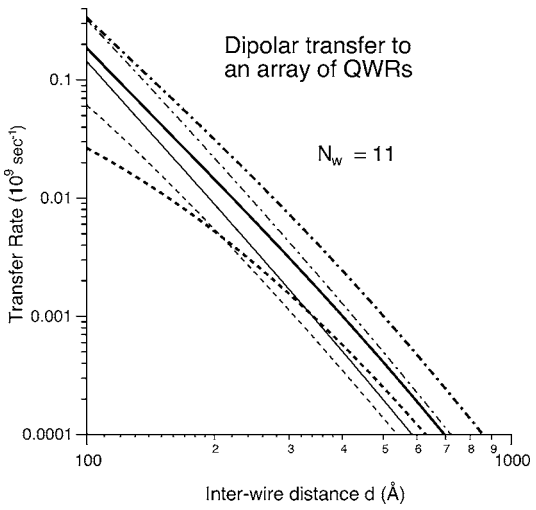

FIG. 11. The total dipolar transfer rate through e-h pair creation for plane-wave (thick curves) and localized (thin curves) excitons from the nQWR to a uniform array of $N_w=11$ parallel wQWRs as a function of the perpendicular distance d for $E_{12}^*=22.6$ meV. The center-to-center separation of the wQWRs is 100 Å. The dipole moments lie in the x (wire) direction for the dashed curve, in the x, y directions for the solid curve, and in the x, y, z directions for the dashed-dotted curve. Other parameters are given in the text.

$=20$ nm, indicating that there is no significant energy transfer beyond $d>15.3$ nm during the lifetime of the exciton. On the other hand, for transfer between two 2D QWs, very efficient transfer was observed for $L_b=13$ nm. Some transfer was observed even for $L_b=20$ nm. While the d-dependence of the rate and the absolute rates are not known, the above 1D-1D result is consistent with the dipolar mechanism of energy transfer but not with the photon-exchange mechanism. Our results in Figs. 2–4 show a lower bound for the transfer time of a few tens of nanoseconds for transfer between the two ground sublevels at a distance $d=150$ Å, much larger than the exciton lifetime of about 0.4 ns measured for a single QWR previously.[13] The above estimated time is somewhat larger than that estimated earlier for 2D-2D transfer between two GaAs QWs with somewhat different parameters.[3] Interestingly, however, the e1h1 transition energy in the nQWR is nearly resonant with the e3h3 energy of the wQWR in their sample, where the PL (photoluminescence) and PLE (photoluminescence excitation) show initially localized excitons.[5] The resonant energy transfer time displayed for this case in Fig. 6 is of the order of a few nanoseconds and may possibly explain the data. There is a caveat, however, that a small net energy mismatch $E_{12}^{**}=1$ meV which is much larger than the inhomogeneous linewidth was employed for the large resonant rate. This may be justified in view of the fact that the inhomogeneous broadening arises from the macroscopic disorder while E_{12}^{**} is influenced only by a locally correlated disorder between neighboring QWRs.

VII. CONCLUSIONS

We have calculated the Stokes exciton transfer rate from a narrow QWR to a wide QWR. Energy transfer through dipole-dipole and photon-exchange coupling was examined. The rate decrease as $1/d^4$ for intermediate d and $1/d^5$ in the asymptotic limit with the distance d for dipolar transfer. For photon-exchange transfer, the rate decreases as $1/d$ in the asymptotic limit. The photon-exchange rate is negligibly small compared with the dipolar rate inside a practical range and dominates the latter only at an extremely long distance where the rates are negligible.

We have also calculated the transfer rate from a narrow QWR to a uniform array of identical parallel wide QWRs as a function of the size of the array and the perpendicular distance d between the narrow QWR and the array. For dipole-dipole transfer, the total transfer rate saturates quickly as the array size grows due to its short range and becomes independent of the array size. Here, the saturated transfer rate decreases as $1/d^4$ with d. On the other hand, the transfer rate increases continuously logarithmically with the size of the array in the asymptotic limit for photon-exchange transfer due to its slow dependence on the range. It also decreases logarithmically with the distance d in the asymptotic limit. The slow range dependence of the transfer rate makes the photon-exchange transfer important in a system consisting of stacks of QWRs and their arrays distributed over a wide range, although the rate between two isolated QWRs is small. The importance of the photon-exchange transfer is also known for energy transfer of Frenkel excitons between optically active impurities in insulators.[16]

Unfortunately, the cited data for transfer between two single QWRs (Ref. 5) show only the quantum efficiency and do not show absolute numerical rates nor their range depen-

dence to compare them directly with the present theoretical predictions. However, the observed transfer efficiency decreases rapidly with the distance d between the two QWRs and was not observable beyond $d=20$ nm in a striking contrast with the case of 2D-2D transfer, where significant transfer is maintained over a range of tens of nanometers[1,2] due to the photon-exchange coupling.[3] The observed rapid range dependence is consistent with our finding. Assuming that significant energy transfer occurs roughly during the lifetime of excitons and that the lifetime is of the order of a nanosecond or shorter, it appears that resonant dipole-dipole transfer rates from e1h1 exciton state of the nQWR to e3h3 exciton of the wQWR best explains the cited data although the theoretical rates may be smaller than the data by about an order of magnitude. Further systematic measurements of the absolute transfer rates and their range dependencies are necessary for a more direct comparison between the theory and the data for the 1D-1D transfer and the transfer from a 1D QWR to an array of 1D QWRs.

The numerical results presented here are expected to become more accurate as the distance between the nQWR and the wQWR becomes much greater than the size of the cross section of the wires. Other key approximations employed in this paper are the effective mass approximation for the hole by neglecting valence band mixing and also the separation of the electron-hole confinement functions in Eq. (31). These approximations affect the exciton binding energy, which enter the 1D density-of-states factor, namely the square root in the denominator of Eq. (26) as well as the resonance factor in the denominator of Eq. (29). The numerical value of the binding energy can be sensitive for the special situation where the binding energies are comparable to the energy mismatch E_{12} to cause resonances for the above quantities. Also, improvement of the exciton wave function in Eq. (31) via variational wave function will bring the electron and the hole closer together, resulting in the increased transfer rate.

ACKNOWLEDGMENTS

The author thanks K. F. Karlsson and H. Weman of Swiss Federal Institute of Technology (EPFL) for calling attention to the problem and for numerous valuable discussions on the subject and their data. The author wishes to thank the faculty of the Physics Department of KAIST for their hospitality, where part of this work was carried out. Sandia is a multiprogram laboratory operated by Sandia Corporation, a Lockheed Martin Company, for the U.S. DOE under Contract No. DE-AC04-94AL85000.

*Permanent address.

[1] A. Tomita, J. Shah, and R. S. Knox, Phys. Rev. B **53**, 10793 (1996).

[2] D. S. Kim, H. S. Ko, Y. M. Kim, S. J. Rhee, S. C. Hohng, Y. H. Yee, W. S. Kim, J. C. Woo, H. J. Choi, J. Ihm, D. H. Woo, and K. N. Kang, Phys. Rev. B **54**, 14580 (1996).

[3] S. K. Lyo, Phys. Rev. B **62**, 13641 (2000).

[4] S. K. Lyo, Phys. Rev. B **64**, 201317(R) (2001).

[5] K. F. Karlsson, H. Weman, S. K. Lyo, K. Leifer, A. Rudra, and E. Kapon, *Proceedings of the 12th International Conference on Modulated Semiconductor Structures (MSS-12)*, July 10–15, 2005, Albuquerque, NM.

[6] T. Takagahara, Phys. Rev. B **31**, 6552 (1985).

[7] Th. Förster, Ann. Phys. **2**, 55 (1948).

[8] Formally, photon-exchange yields dipole-dipole coupling at a short distance.

[9] Y. C. Chang, L. L. Chang, and L. Esaki, Appl. Phys. Lett. **47**, 1324 (1985).

[10] Equation (2.5) in Ref. 3 has a typographical error and should read $G(\mathbf{R}_\parallel)=\exp(-R_\parallel^2/2\xi^2)/\xi\sqrt{\pi}$. The subsequent results are not affected.

[11] D. L. Dexter, J. Chem. Phys. **21**, 836 (1953).

[12] Equation (3.24) of Ref. 3 can also be derived from Eqs. (22) and (23).

[13] D. Y. Oberli, M.-A Dupertuis, F. Reinhardt, and E. Kapon, Phys. Rev. B **59**, 2910 (1999).

[14] P. Thomas, M. Möller, R. Eichmann, T. Meier, T. Stroucken, and A. Knorr, Phys. Status Solidi B **230**, 25 (2002).

[15] A. C. G. Mitchell and M. W. Zemansky, *Resonance and Excited Atoms* (Cambridge University Press, Cambridge, England, 1961), p. 99.

[16] T. Holstein, S. K. Lyo, and R. L. Orbach, Phys. Rev. B **16**, 934 (1977).